RISK ASSESSMENT OF EROSION FROM CONCENTRATED FLOW ON RANGELANDS USING OVERLAND FLOW DISTRIBUTION AND SHEAR STRESS PARTITIONING

O. Z. Al-Hamdan, F. B. Pierson, M. A. Nearing, C. J. Williams, J. J. Stone, P. R. Kormos, J. Boll, M. A. Weltz

ABSTRACT. *Erosion rates of overland flow on rangelands tend to be relatively low, but under certain conditions where flow is concentrated, soil loss can be significant. Therefore, a rangeland site can be highly vulnerable to soil erosion where overland flow is likely to concentrate and exert high shear stress on soil grains. This concept is commonly applied in cropland and wildland soil erosion modeling using predictions of flow effective shear stress (shear stress applied on soil grains). However, historical approaches to partition shear stress in erosion models are computationally complex and require extensive parameterization. Furthermore, most models are not capable of predicting the conditions in which concentrated flow occurs on rangelands. In this study, we investigated the rangelands conditions at which overland flow is more likely to become concentrated and developed equations for partitioning the shear stress of concentrated flow on rangelands. A logistic equation was developed to estimate the probability of overland flow to become concentrated. Total shear stress of rangeland overland flow was partitioned into components exerted on soil, vegetation, and rock cover using field experimental data. In addition, we investigated the vegetation cover limit at which the effective shear stress component is substantially reduced, limiting the erosion rate. The results from the partitioning equations show that shear stress exerted on soil grains was relatively small in sheet flow. Shear stress exerted on soil grains in concentrated flow was significantly higher when bare soil exceeded 60% of the total surface area but decreased significantly when the bare soil area was less than 25% or when the plant base cover exceeded 20%. These percentages could be used as relative measures of hydrologic recovery for disturbed rangelands or as triggers that indicate a site is crossing a threshold beyond which soil erosion might accelerate due to the high effective shear stress.*

Keywords. *Concentrated flow, Fire impact, Overland flow, Rangeland, Shear stress partitioning, Sheet flow, Soil erosion modeling.*

Erosion rates on rangelands tend to be relatively low, but under certain conditions soil loss can be significant. On most undisturbed rangelands, soil loss is minimal and occurs primarily by rain splash and sheet erosion. However, concentrated flow is commonly the dominant mechanism of water erosion following disturbance on steep slopes or where ground cover is sparse (Pierson et al., 2009, 2011).

Rates of soil erosion caused by overland flow runoff are controlled by soil detachment and transport processes. The main hydraulic variables that control these processes are flow rate and velocity, slope gradient, and the cross-sectional geometry of the flow. Physically based models combine some or all of these variables into one or more composite hydraulic variables to predict soil detachment and transport capacity. One of these composite hydraulic variables often used is the flow shear stress (Einstein and Banks, 1950; Foster, 1982; Foster et al., 1982). Flow shear stress (τ_t, N m^{-2}) can be calculated using the following equation:

$$\tau_t = \gamma R_h \sin\left(\tan^{-1}\left(S\right)\right) \quad (1)$$

where

γ = specific weight of water (N m^{-3})
R_h = hydraulic radius of the flow (m)

Submitted for review in April 2012 as manuscript number SW 9751; approved for publication by the Soil & Water Division of ASABE in February 2013. Presented at the 2011 Symposium on Erosion and Landscape Evolution (ISELE) as Paper No. 11134.

The authors are **Osama Z. Al-Hamdan,** Research Associate, and **Frederick B. Pierson,** Research Leader, USDA-ARS Northwest Watershed Research Center, Boise, Idaho; **Mark A. Nearing, ASABE Member,** Research Agricultural Engineer, USDA-ARS Southwest Watershed Research Center, Tucson, Arizona; **Christopher Jason Williams,** Hydrologist, USDA-ARS Northwest Watershed Research Center, Boise, Idaho; **Jeffry J. Stone, ASABE Member,** Research Hydrologist, USDA-ARS Southwest Watershed Research Center, Tucson, Arizona; **Patrick R. Kormos,** Graduate Student, Department of Geosciences, Boise State University, Boise, Idaho; **Jan Boll, ASABE Member,** Professor, Department of Biological and Agricultural Engineering, University of Idaho, Moscow, Idaho; and **Mark A. Weltz, ASABE Member,** Research Leader, USDA-ARS Great Basin Rangelands Research Unit, Reno, Nevada. **Corresponding author:** Osama Z. Al-Hamdan, USDA-ARS Northwest Watershed Research Center, 800 E. Park Blvd, Plaza IV, Suite 105, Boise, ID 83712; phone: 208-422-0706; e-mail: osama.al-hamdan@ars.usda.gov.

S = slope (m m^{-1}).

On bare soil surfaces, shear stress is exerted on soil grains or soil form roughness; however, on surfaces with rock and vegetation cover, the shear stress is exerted on the entire composite surface (Einstein and Banks, 1950). In many physically based models, only overland flow shear stress exerted on soil aggregates (grains) is used to estimate soil detachment rate and sediment transport capacity. For instance, the Water Erosion Prediction Project (WEPP) model (Nearing et al., 1989; Flanagan and Nearing, 1995) uses the following equation to estimate soil detachment rate:

$$D_r = K_r\left(\tau_e - \tau_c\right)\left(1 - \frac{G}{T_c}\right) \tag{2}$$

where

D_r = rill detachment rate (kg s^{-1} m^{-2})

K_r = rill erodibility parameter (s m^{-1})

τ_e = effective flow shear stress acting on the soil (N m^{-2})

τ_c = critical shear stress at which soil detachment initiates (N m^{-2})

G = sediment load (kg s^{-1} m^{-1})

T_c = sediment transport capacity (kg s^{-1} m^{-1}).

The transport sediment capacity is calculated by the following equation:

$$T_c = k_t \tau_e^{1.5} \tag{3}$$

where k_t is a transport coefficient (m$^{0.5}$ s^2 kg$^{-0.5}$). Equations 2 and 3 are largely dependent on, and hence need a good estimate of, the partitioned shear (τ_e) in order to perform well. Equation 1 estimates only the total shear stress; therefore, partitioning of the calculated total shear stress into components exerted on soil, vegetation cover, and rock cover is a key element for advancing erosion predictive technologies such as WEPP.

Multiple approaches have been reported in the literature that separate the effective shear stress exerted on soil grains from the total shear stress (e.g., Giménez and Govers, 2008). Foster (1982) estimated the effective shear stress component based on the assumption that the ratio of effective shear stress to total shear stress is equal to the ratio of the soil hydraulic friction factor to the friction factor of the composite surface:

$$\frac{\tau_e}{\tau_t} = \frac{f_s}{f_t} \tag{4}$$

where f_s and f_t are the Darcy-Weisbach hydraulic friction factor of the soil and the hydraulic friction factor of the composite surface, respectively. This method is based on the theory that the grain friction factor is independent of the presence of form shear stress, and thus the total hydraulic resistance can be divided into that which occurs because of the soil grains and that which occurs because of form roughness (Einstein and Banks, 1950; Einstein and Barbarossa, 1952).

A second method uses the measured mean velocity of the flow to estimate the corresponding hydraulic radius on a plane bed, which is then used to calculate the grain shear stress (Laursen, 1958; Foster et al., 1980, 1982):

$$\tau_e = \gamma R_{hs} \sin\left(\tan^{-1}\left(S\right)\right) \tag{5}$$

where R_{hs} is the effective hydraulic radius due to soil. Foster et al. (1982) used Manning's equation to calculate R_{hs} as:

$$R_{hs} = \left(\frac{V \mathrm{n}_s}{S^{0.5}}\right)^{1.5} \tag{6}$$

where V is flow velocity (m s^{-1}), and n_s is Manning's n of a plane bed.

Raupach (1992) proposed using drag force partitioning theory to predict shear stress portions. Even though originally developed to deal with wind shear stress, Thompson et al. (2004) showed that Raupach's method is applicable to runoff shear stress by:

$$\frac{\tau_e}{\tau_t} = \frac{C_p}{C_p + C_R \lambda} \tag{7}$$

where

C_p = soil particle drag coefficient

C_R = drag coefficient for a single vegetal element

λ = roughness density, which is related to the number and size of vegetal elements per surface area.

Temple (1980, 1983, 1985) also applied the concept of separating the effective shear stress from the total shear stress for the purpose of designing vegetated channels. With the assumption that vegetal cover is dense and uniform, Temple (1980) derived the following equation for calculating the effective shear stress:

$$\frac{\tau_e}{\tau_t} = \left(1 - C_F\right)\left(\frac{\mathrm{n}_s}{\mathrm{n}}\right)^2 \tag{8}$$

where

C_F = empirical parameter describing the potential of the vegetal cover to dissipate turbulence eddies in the immediate vicinity of the soil/water boundary

n_s = Manning's n resistance coefficient associated with the soil only

n = Manning's n resistance coefficient for the channel.

Foster's (1982) approach has been commonly applied in physically based erosion models such as WEPP (Nearing et al., 1989) and CREAMS/GLEAMS (Foster et al., 1980) where the friction factor is accounted separately for the different effects of cover. In order to apply this method, the friction factor must be partitioned by surface elements. Several methods have been developed for partitioning the friction factor (e.g., Weltz et al., 1992; Gilley and Weltz, 1995; Hu and Abrahams, 2006; Wilcox et al., 2006; Li, 2009), but most of these approaches are difficult to implement in existing field-scale erosion models due to their high computational and input demands. Although some data have been reported in the past related to shear stress partitioning for natural lands and rangelands (e.g., Weltz et al., 1992), most of the reported data were

collected either in the laboratory (e.g., Li, 2009) or in row-crop agricultural settings (e.g., Gilley and Weltz, 1995; Giménez and Govers, 2008).

The objectives of this study are: (1) to investigate cover and flow conditions under which flow transitions from sheet to concentrated flow, thereby identifying the limit at which the effective shear stress component is substantially increased, thus accelerating the potential erosion rate, and (2) to develop equations that estimate the effective overland flow shear stress by applying the Darcy-Weisbach friction partitioning method to field-collected experimental data for rangelands.

MATERIALS AND METHODS

STUDY SITES

The data used in this study were obtained from rangeland field experimental work by the USDA-ARS Northwest Watershed Research Center in Boise, Idaho. The work resulted in hundreds of experimental plots. The data were collected from rangeland sites within the U.S. Great Basin region and span a wide range of slope angles (5.6% to 65.8%), soil types, and vegetative cover (table 1). Many of the sites exhibit some degree of disturbance and/or treatments, such as tree encroachment, wildfire, prescribed fire, tree mastication, and/or tree cutting (table 1). Numerous rectangular plots (approx. 4 m long × 2 m wide) were selected at each site, encompassing all treatments for the respective site. Average slope, canopy and ground cover, and microtopography were measured for each plot (Pierson et al., 2007, 2009, 2010).

MEASUREMENT AND CALCULATION OF HYDRAULIC PARAMETERS AND EROSION RATE

Overland flow was simulated on each experimental plot for a range of flow rates over near-saturated surface soil conditions. Surface soils were pre-wetted by artificial rainfall immediately prior to overland flow initiation (Pierson et al., 2007, 2008a, 2009). Overland flow was released from a concentrated source centered 4 m upslope of the plot discharge outlet (Pierson et al., 2007, 2008a, 2009, 2010; Moffet et al., 2007). Each inflow rate was applied for 12 min using a flow regulator. In the early experiments (before 2006), the applied inflow rates were 3, 7, 12, 15, 21, 24 L min^{-1}, while they were 15, 30, 45 L min^{-1} in the later experiments, with the exception of the Breaks site in 2004. The plot flow velocity for each inflow rate was measured using a salt ($CaCl_2$) tracing method. A concentrated salt solution was released into the fastest (as determined by visual tracer) flow path. The mean travel time of the salt solution between rill cross-sections at transects 1 and 3 m downslope of the release point was monitored instantaneously with conductivity probes. Flow velocity was calculated as the distance between conductivity probes (2 m) divided by the mean travel time of the salt solution between the 1 and 3 m transects. Flow width and depth measurements at transects 1 and 3 m downslope of the flow release were used in this study, in order to be consistent with the velocity measurements. Flow dimension measurements at some sites were taken at transects 0.5, 1.5, 2.5, 3.5 m. In these cases, only dimension measurements at 1.5 and 2.5 m were considered (Al-Hamdan et al., 2012). For flow path calculations, each flow path cross-section was assumed to be rectangular in order to achieve consistency in the data analyses (Al-Hamdan et al., 2012). Multiple depth measurements were taken for each cross-section, and the depth was calculated as the average of these measurements. The average width, depth, and hydraulic radius (R_h) of each flow path for each inflow rate was then calculated as the average of means from each cross-section. The hydraulic radius was calculated as:

$$R_h = \frac{A}{P_{wet}} \tag{9}$$

where A is the cross-sectional area (m^2), and P_{wet} is the wetted perimeter (m). In the rectangular cross-section case, R_h was calculated as:

$$R_h = \frac{wd}{(w+2d)} \tag{10}$$

where w and d are the average width and the average depth of each flow path, respectively (m).

Experimental runs resulted in two runoff categories: concentrated flow runs and sheet flow runs. Concentrated flow paths were separated from sheet flow by comparing the hydraulic radius to the flow depth for the respective flow path (Al-Hamdan et al., 2012). If the flow path was too shallow, the depth of the flow would be negligible with respect to the width. In this case, the denominator in equation 10 would be approximately equal to w, and R_h would be approximately equal to d. In our data, if R_h and d were significantly different (i.e., d is 5% or more greater than R_h), then the flow path was considered as concentrated flow. In some cases, the flow would be concentrated at the top of the plot due to scouring at the inflow release point and then start to disperse downhill, changing to sheet flow. In order to avoid considering such cases as concentrated flow or sheet flow, the criterion was applied on each path at transects 1 and 3 m from the top of the plot. In

Table 1. Land management treatments, dominant plant community, and soil type descriptions for rangeland field sites in this study.

Site	State	Treatment	Landscape	Soil Type
Denio	Nevada	Burned, untreated	Sagebrush steppe	Sandy loam
Breaks	Idaho	Burned, untreated	Sagebrush steppe	Course sandy loam
Steens	Oregon	Cut, uncut	Western juniper	Silt loam
Onaqui	Utah	Burned, tree mastication, cut, untreated	Sagebrush steppe/Utah juniper	Gravely loam
Marking corral	Nevada	Burned, cut, untreated	Pinyon-juniper/sagebrush steppe	Gravelly loam
Castlehead	Idaho	Burned, cut, untreated	Western juniper/sagebrush steppe	Stony loam
Upper Sheep	Idaho	Burned, untreated	Sagebrush steppe	Silt or silt loam

experimental runs that formed concentrated flow paths and sheet flow at the same time, the case was considered as concentrated flow only if the flow path that had the largest hydraulic radius was concentrated. After categorizing the experimental runs into concentrated flow runs and sheet flow runs, the hydraulic parameters were calculated using the calculated depth of the cross-section from the measured flow discharge, flow velocity, and flow width instead of the field-measured depth (Al-Hamdan et al., 2012).

The overland flow discharge for each experimental run was calculated as the average of the inflow rate and the outflow rate of a plot. While the inflow rate was controlled and measured by the flow regulator, the outflow discharge rate was derived from timed runoff samples that were collected in bottles or buckets at the exit of the plot (Pierson et al., 2007, 2009, 2010). The outflow discharge rate was calculated as the sample volume divided by the collection time. The timed runoff samples were weighed, oven-dried at 105°C, and then re-weighed to estimate the runoff sediment concentration.

In order to find the flow discharge in the flow path that corresponded to the measured velocity, the total overland flow discharge was distributed to the flow paths based on their hydraulic radius. Manning's equation was used for calculating the conveyance factor (K) for each component, and then the total flow rate was distributed proportionally to each channel component based on its K value (Al-Hamdan et al., 2012). For instance, an individual flow path with twice the conveyance factor as a second flow path would have twice the share of the collective flow.

To calculate the effective shear stress, we followed Foster's (1982) method of partitioning the friction factor by combining equations 1 and 4:

$$\tau_e = \gamma R_h \sin\left(\tan^{-1}(S)\right)\left(\frac{f_s}{f_t}\right) \tag{11}$$

The measured Darcy-Weisbach friction factor (f_t) was calculated by:

$$f_t = \frac{8gR_hS}{V^2} \tag{12}$$

where

V = measured velocity (m s^{-1})

S = average slope of the plot (m m^{-1})

g = acceleration due to gravity (m s^{-2})

R_h = hydraulic radius (m).

Empirical equations that predict the measured total friction factor (f_t) were developed by regressing the measured total friction against the measured vegetation and rock cover, slope, and flow rate (Al-Hamdan et al., 2012). In order to estimate the friction factor of soil grains, the vegetation cover term was assumed as the friction contribution to the total friction factor. The soil hydraulic friction portion was assumed to be the logarithmic difference between the total friction and the friction of the cover elements. The intercept in the equation was assumed to be the friction factor due to soil grains. Flow discharge and slope were used to track the temporal and spatial variability of the ratio of soil roughness to total hydraulic roughness, given that the temporal variability of flow discharge and the spatial variability of slope were available. Equation 4 was then used to find the effective shear stress.

In order to examine the difference in hydraulics regimes between the concentrated flow and sheet flow data, the relationship between the total friction and Reynolds number (Re) was investigated. Reynolds number was calculated by the following equation:

$$\mathrm{Re} = \frac{4VR_h}{\upsilon} \tag{13}$$

where υ is the kinematic viscosity (m^2 s^{-1}).

Statistical Analysis

SAS software (SAS, 2007) was used for all statistical analyses. Simple linear regression analysis was used to test the relationship between the hydraulic friction (f_t) and Reynolds number and to test the relationship between the sediment flux and shear stress. Multiple stepwise linear regression analysis was used to derive all the relationships between the hydraulic friction (f_t) as dependent variable and ground cover attributes, slope, and flow discharge as independent variables. In addition to ordinary least squares (OLS) regression, reduced major axis (RMA) regression was used to develop the relationship between the hydraulic friction (f_t) as dependent variable and ground cover. Prior to regression analysis, values of variables were log transformed (base 10) to address deviation from normality as well as to improve the uniformity of variance and linearity (Allison, 1999). The general linear model was used to test the significance of differences between relationships among runoff categories. Logistic regression analysis was used to develop a model that predicts the probability of concentrated flow formation in overland flow based on bare soil fraction, slope, and unit flow discharge values. A significance level of 0.05 was used for all statistical tests, including the criteria for including the variables in the multiple regressions.

Results and Discussion

Concentrated Flow and Sheet Flow

The results show that formation of concentrated flow was positively correlated with flow discharge per unit width, slope, and ground cover. For instance, for sites with relatively gentle slope (i.e., slope is less than 0.2) at an inflow rate of 30 L min^{-1}, only 14% of the experimental runs were concentrated flow. This number increased to 46% for steep-slope experiential runs (i.e., slope is larger than 0.2) at the same inflow rate. Concentrated flow was generated in 41% of the experimental runs performed on plots with less than 25% bare soil. The percentage of experimental runs that generated concentrated flow doubled to 80% on plots with more than 75% bare soil.

A multiple logistic regression that predicts the probability of overland flow to concentrate (P) was developed:

$$P = \frac{\exp(-6.397 + 8.335S + 3.252bare + 3440q)}{1 + \exp(-6.397 + 8.335S + 3.252bare + 3440q)} \quad (14)$$
$$(n = 756)$$

where

S = slope (m m^{-1})

bare = fraction of bare soil to total area (m^2 m^{-2})

q = flow discharge per unit width (m^2 s^{-1}).

The ranges of S, *bare*, and q used for developing the equation were 0.06 to 0.57, 0 to 0.95, and 0.27 × 10^{-4} to 57.13 × 10^{-4} m^2 s^{-1}, respectively. The equation takes into account the three major drivers of concentrated flow formation (flow discharge, bare soil fraction, and slope angle). A larger unit flow discharge indicates a larger hydraulic radius, which increases the chances for flow to be concentrated. Infiltration rates are generally high in vegetated or litter-covered areas on rangelands, whereas bare ground promotes rapid runoff generation (Blackburn, 1975; Pierson et al., 1994; Wilcox et al., 1997; Ludwig et al., 2005; Pierson et al., 2007, 2008b, 2009, 2010). Interconnected bare ground patches increase the continuity of overland flow paths, which amplifies flow velocity and depth by reducing hydraulic friction, leading to concentrated flow formation (Abrahams et al., 1995, Parsons et al., 1996; Ludwig et al., 2005; Pierson et al., 2007; Al-Hamdan et al., 2012). These effects are exacerbated by steep terrain (Al-Hamdan et al., 2012), although infiltration and slope steepness have been shown to have a positive correlation on some rangelands (Wilcox et al., 1988).

HYDRAULIC FRICTION

In general, total friction factor (f_t) was higher in the concentrated flow cases than in the sheet flow cases. Total friction factor was correlated negatively with Reynolds number (Re) in concentrated flow (fig. 1). On the other hand, the (f_t – Re) relationship was not significant in sheet flow (α = 0.05). The negative correlation between f_t and Re in the concentrated flow data verifies the assumption that these data were obtained from concentrated flow experiments where total submergence is predominant in the flow path (Al-Hamdan et al., 2012). The insignificance of the (f_t – Re) relationship in the sheet flow case can be explained by the fact that resistance increases with flow rate as the wetted surface area increases, and resistance starts to decrease with Re after total submergence (Abrahams et al., 1995).

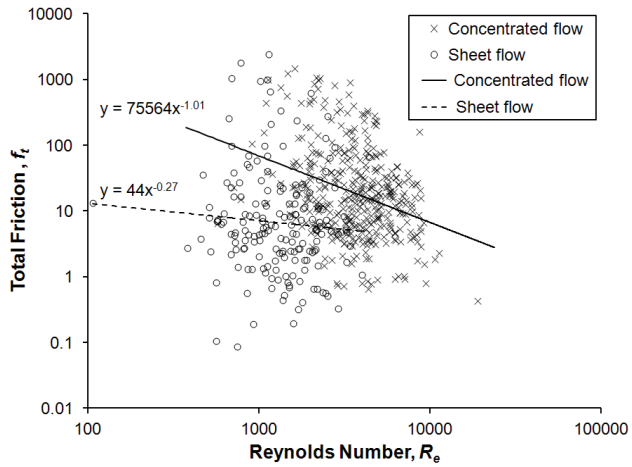

Figure 1. Darcy-Weisbach total friction factor (f_t) as a function of Reynolds number (Re) for concentrated flow and sheet flow data.

Total hydraulic friction was negatively correlated with flow discharge and the percentage of bare ground and was positively correlated with the presence of vegetation cover and slope. Equations that were developed from concentrated flow data have significantly different coefficient values compared to those obtained from sheet flow data (eqs. 15 through 25 in table 2). The flow discharge and slope in the total friction equation improved the prediction of the total friction and thus improved the prediction of the proportion of the assumed soil friction to total friction (table 2). Adding the slope and flow discharge variables to the regression improved the prediction of the equations for both concentrated flow and sheet flow, as the coefficient of determination (R^2) increased from 0.44 in equation 15 to 0.51 in equation 18 and from 0.51 in equation 19 to 0.55 in equation 21. All equations in table 2 show that the basal plant cover term has the greatest effect on total friction among other cover attributes. The influence of cover attributes on total friction factor is more evident for the sheet flow case. For instance, the impact of basal plant cover on the logarithm total friction in the sheet flow case (eq. 20) is twice its impact in the concentrated flow case (eq. 16).

Equations 15 and 19 can be approximated by combining all cover attributes into one cover variable (*cover*). This approximation resulted into the following equation for concentrated flow:

$$\log(f_t) = 0.55 + 1.51 cover \quad (n = 171, R^2 = 0.31) \quad (26)$$

and the following equation for sheet flow:

$$\log(f_t) = -0.35 + 2.14 cover \quad (n = 101, R^2 = 0.33) \quad (27)$$

SHEAR STRESS PARTITIONING

Equations 15 through 21 were used to develop empirical equations that predict the ratio of effective shear stress to the total shear stress (τ_e/τ_t) of concentrated flow and sheet flow as a function of cover attributes (table 3). The (τ_e/τ_t) ratio calculated using these equations was also regressed against bare soil fraction area. Figure 2 shows the developed equations for concentrated flow using equations 15 and 18. As can be seen in figure 2, adding the slope and flow discharge in equations 18 improved the relation between shear stress fraction and percent bare soil fraction to total area. It can be seen that, in the case of using equation 15, few points deviated from the general trend. The deviation of these points could be because rock cover has high influence in the sites from where these data

Table 2. Empirical equations for predicting f_t for different flow categories as a function of fraction of litter cover (*res*), fraction of basal plant and cryptogam cover (*bascry*), fraction of rock cover (*rock*), slope (*S*), and flow discharge, (*Q*, m^3 s^{-1}).

Flow	Equation	Statistics	Equation No.
Concentrated	$\log(f_t) = 0.543 + 1.619res + 1.838bascry$	n = 171, R^2 = 0.44	15
	$\log(f_t) = 0.015 + 1.393res + 1.57bascry + 1.955S$	n = 171, R^2 = 0.54	16
	$\log(f_t) = 0.846 + 1.416res + 1.759bascry - 1444Q$	n = 391, R^2 = 0.45	17
	$\log(f_t) = 0.250 + 1.349res + 1.763bascry + 1.339rock - 1519Q + 1.715S$	n = 391, R^2 = 0.51	18
Sheet	$\log(f_t) = -0.165 + 2.044res + 3.133bascry + 0.955rock$	n = 101, R^2 = 0.51	19
	$\log(f_t) = -0.048 + 2.324res + 3.212bascry + 1.263rock - 1207Q$	n = 178, R^2 = 0.53	20
	$\log(f_t) = -0.196 + 2.20res + 2.293bascry + 1.188rock - 1224Q + 1.648S$	n = 178, R^2 = 0.55	21
All	$\log(f_t) = 0.413 + 1.493res + 2.254bascry$	n = 390, R^2 = 0.44	22
	$\log(f_t) = -0.109 + 1.425res + 0.442rock + 1.764bascry + 2.068S$	n = 390, R^2 = 0.53	23
	$\log(f_t) = 0.731 + 1.525res + 2.076bascry - 1424Q$	n = 756, R^2 = 0.50	24
	$\log(f_t) = 0.141 + 1.53res + 1.902bascry + 0.783rock - 1224Q + 1.732S$	n = 756, R^2 = 0.56	25

Table 3. Empirical equations for predicting friction due to soil (f_s) and the ratio of the hydraulic friction factor of the soil to the friction factor of the composite surface (f_s/f_t) based on equations 15 through 25 (in table 2) for different flow categories as a function of fraction of litter cover (*res*), fraction of basal plant and cryptogam cover (*bascry*), fraction of rock cover (*rock*), slope (*S*), and flow discharge (*Q*, m^3 s^{-1}).

Flow	$\log(f_s)$	$\log(f_s/f_t)$	Corresponding f_t Equation No.
Concentrated	0.543	$-1.619res - 1.838bascry$	15
	$0.015 - 1.955S$	$-1.393res - 1.57bascry$	16
	$0.846 - 1444Q$	$-1.416res - 1.759bascry$	17
	$0.250 - 1519Q + 1.715S$	$-1.349res - 1.763bascry - 1.339rock$	18
Sheet	−0.165	$-2.044res - 3.133bascry - 0.955rock$	19
	$-0.048 - 1207Q$	$-2.324res - 3.212bascry - 1.263rock$	20
	$-0.196 - 1224Q + 1.648S$	$-2.20res - 2.293bascry - 1.188rock$	21
All	0.413	$-1.493res - 2.254bascry$	22
	$-0.109 + 2.068S$	$-1.425res - 1.764bascry - 0.442rock$	23
	$0.731 - 1424Q$	$-1.525res - 2.076bascry$	24
	$0.141 - 1224Q + 1.732S$	$-1.53res - 1.902bascry - 0.783rock$	25

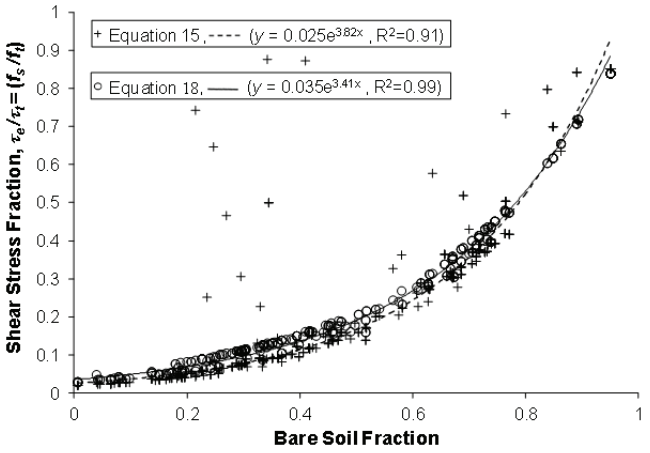

Figure 2. Empirical equations that predict the ratio of effective shear stress to total shear stress (τ_e/τ_t) of concentrated flow as a function of the bare soil fraction of the total area based on equations 15 and 18.

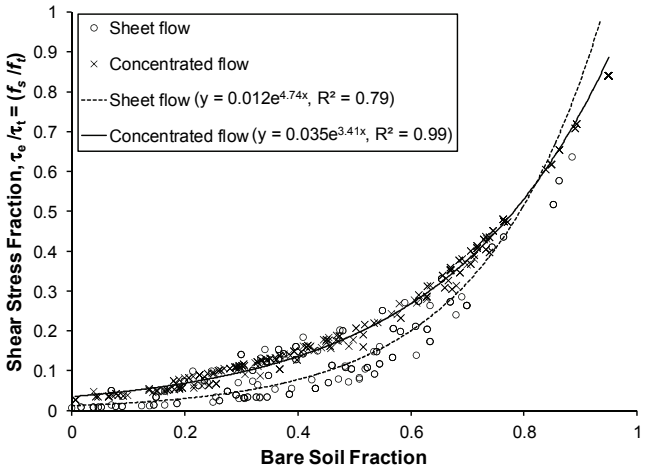

Figure 3. Empirical equations that predict the ratio of effective shear stress to the total shear stress (τ_e/τ_t) of sheet flow and concentrated flow as a function of bare soil fraction of total area based on equations 18 and 21.

points were taken. Rock cover did not show up in the multiple regressions in equation 15; therefore, using bare soil fraction as a surrogate variable for all cover attributes would not work in sites with high rock cover.

Figure 3 shows shear stress partitioning equations for concentrated flow and sheet flow using equations 18 and 21, respectively. As can be seen, when plots have less than 80% bare soil, the ratio of effective shear stress to total shear stress is higher in concentrated flow. The lower effective shear stress fraction at the same bare soil values indicates that ground cover has more influence in protection of soil in the case of sheet flow.

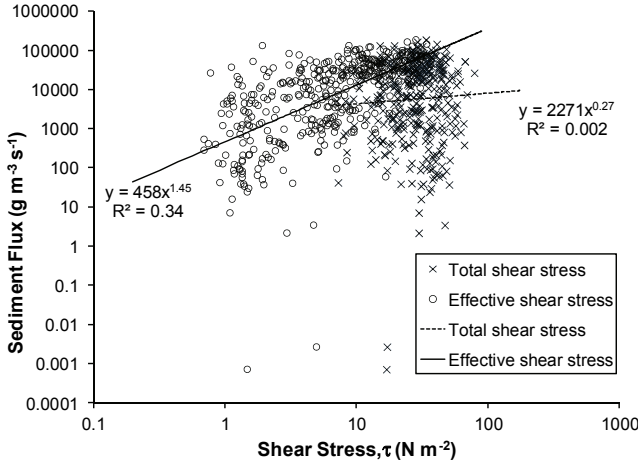

Figure 4. Relationship between sediment flux as a dependent variable and total shear stress and effective shear stress using equation 18 as independent variables.

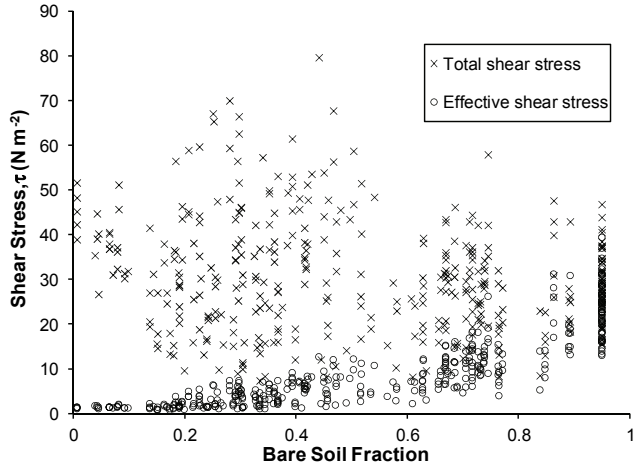

Figure 5. Total shear stress and effective shear stress estimated by equation 18 as a function of bare soil fraction.

The relationship between total shear stress and soil sediment flux was not significant (fig. 4). On the other hand, the effective shear stress estimated by equation 18 is significantly correlated with soil sediment flux. Even though the relationship in figure 4 was developed using data from several sites with different erodibilities, the results emphasize the importance of partitioning the shear stress in order to make it a useful erodibility predictor.

In general, total shear stress was higher in concentrated flow cases, as they have a larger hydraulic radius. Figure 5 shows the total shear stress and effective shear stress portion as a function of bare soil using equation 18. Regardless of the value of total shear stress, the shear stress exerted on soil grains in the concentrated flow case estimated by equation 18 was significantly higher when the bare soil percentage exceeded 60% and significantly lower when bare soil was less than 25%. The same trend is evident in figure 6, where effective shear stress as an average is relatively small, regardless of the total shear stress value, when the basal plant cover exceeds 20%. In general, total shear stress in sheet flow was relatively small, except in plots that were fully covered (fig. 7). Effective

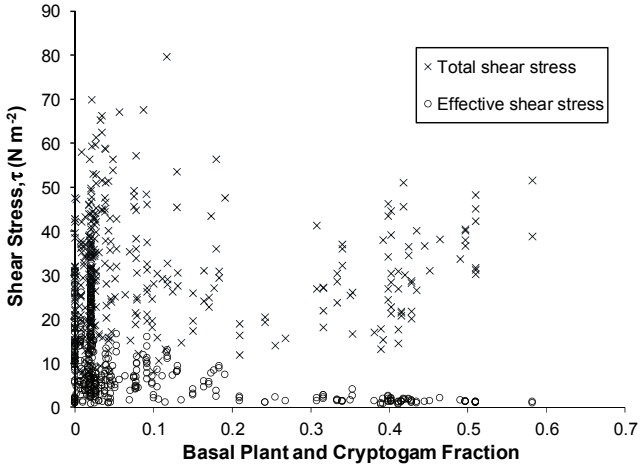

Figure 6. Total shear stress and effective shear stress estimated by equation 18 as a function of basal plant and cryptogam fraction.

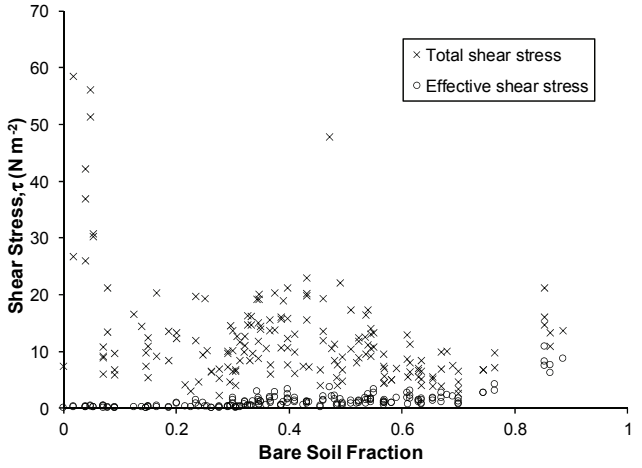

Figure 7. Total shear stress and effective shear stress estimated by equation 21 as a function of bare soil fraction.

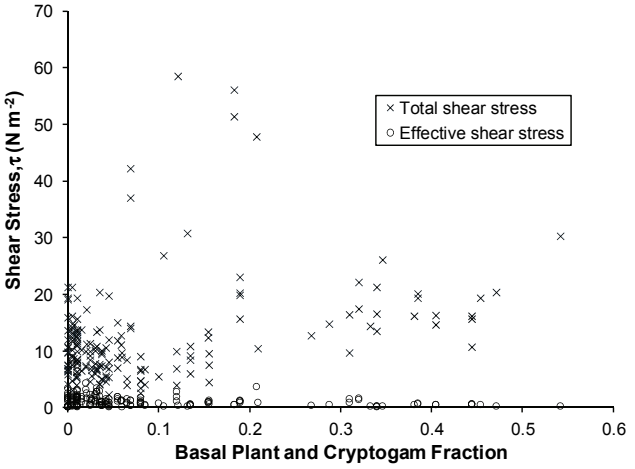

Figure 8. Total shear stress and effective shear stress estimated by equation 21 as a function of basal plant and cryptogam fraction.

shear stress in the sheet flow case estimated by equation 21 was very small, except when bare soil exceeded 80%. Effective shear stress was also relatively small in the sheet flow case, regardless of the total shear stress value, except when the basal plant cover was totally absent (fig. 8). The

relatively low values of hydraulic radius in the sheet flow case explain why total shear stress, as calculated by equation 1, is low. The low total shear stress in the sheet flow experiments can also be explained by the fact that the sheet flow cases occurred on gently sloped plots. If the plots had a steep slope, then the flow would have likely been concentrated, unless the plots were fully covered. In that case, the shear stress would have been high, but mostly applied on the cover and not the soil grains.

RMA REGRESSION

The equations presented in table 2 were developed using OLS regression. OLS regression can sometimes underestimate the slope and overestimate the intercept of the regression. In order to see how using OLS regression impacted our results, we also applied RMA regression to develop equations similar to equations 26 and 27. The equations resulting from the RMA regression were as follows for concentrated flow:

$$\log(f_t) = -0.08 + 2.7\,cover \tag{28}$$

and for sheet flow:

$$\log(f_t) = -1.33 + 3.73\,cover \tag{29}$$

Figure 9 shows the regression results between log-transformed total friction and ground cover for concentrated flow using OLS and RMA regressions (i.e., eqs. 26 and 28). It can be seen that, as expected, OLS regression underestimated the slope of the regression (i.e., hydraulic friction explained by cover) and overestimated the intercept (i.e., friction due to soil grain). Figure 10 shows the shear stress partitioning equations based on equations 26 and 28 for concentrated flow. It can be seen that the estimate of the fraction of effective shear stress to total shear stress was dramatically reduced when using RMA regression. These estimates indicate that the fraction of effective shear stress can be negligible until the bare soil fraction exceeds 60%. This conclusion is more evident in figure 11, where estimates of effective shear stress using RMA regression for the concentrated flow experiments are depicted. Figure 11 also shows the effective shear stress estimates using OLS regression (i.e., eq. 26). It can be seen that, even though the OLS values are higher than those from RMA regression, the same conclusion holds, i.e., effective shear stress cannot be negligible when the bare soil fraction exceeds 60%. This corroborates Gifford's (1985) extensive review of the literature on rangeland cover, which concluded that ground cover should be maintained above a critical threshold of ~50% to adequately protect the soil surface.

Using RMA in equations 28 and 29 might give better estimates for shear stress partitioning, since the coefficient of determination when using only cover as an independent variable in equations 26 and 27 was very low. However, using OLS regression in these equations can be reasonable, as the coefficient of determination of empirical equations 18 and 21 was higher. In addition, OLS regression would be even more reasonable if the purpose of the shear stress partitioning is risk assessment, since OLS gives higher estimates of the effective shear stress than RMA, and thus gives more confidence for decisions to protect a vulnerable rangeland site.

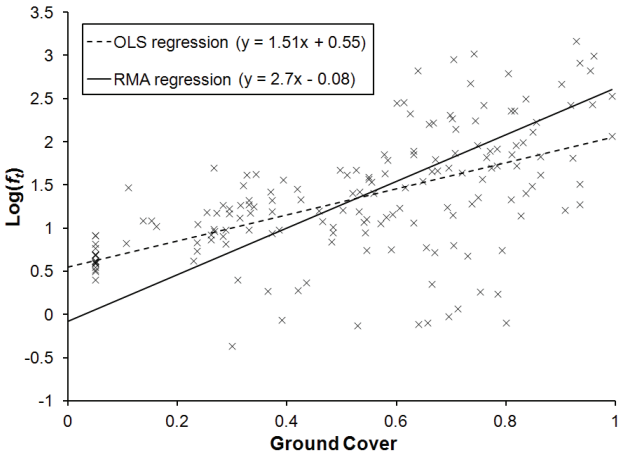

Figure 9. Log-transformed total friction factor log(f_t) in concentrated flow as a function of ground cover using OLS and RMA regression.

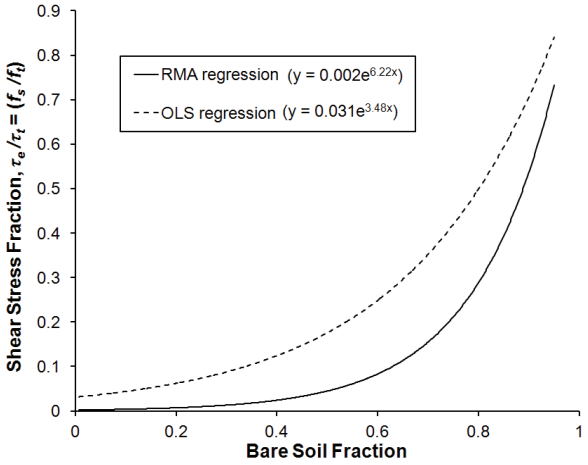

Figure 10. Empirical equations that predict the ratio of effective shear stress to total shear stress (τ_e/τ_t) of concentrated flow as a function of the bare soil fraction of the total area based on equations 26 and 28.

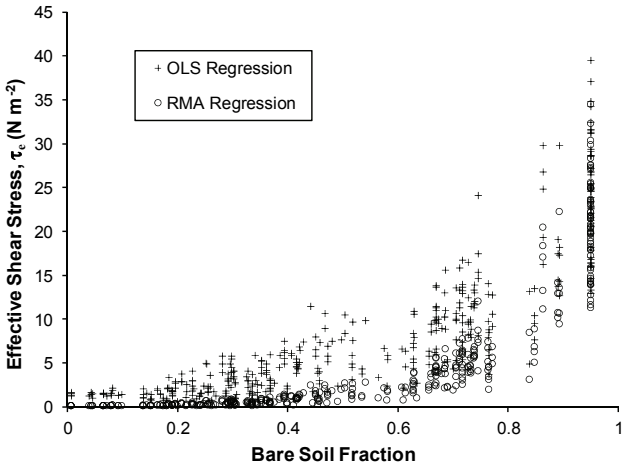

Figure 11. Effective shear stress estimated by equation 26 (OLS regression) and equation 28 (RMA regression) as a function of the bare soil fraction.

IMPLICATIONS

The resulting predictive equations in this study were obtained from data that represent a diverse set of rangeland environments. In addition, these predictive equations were developed from a data set with high variability of the hydraulic regime (e.g., Reynolds number varied from 106 to 18,915). Such high variability within the data set makes the resulting predictive equations applicable to a wide range of flow regimes, ecological sites, soils, slopes, and vegetation and ground cover conditions. Therefore, these equations could be used to improve the performance of physically based hydrology and erosion models, as well as the performance of erosion risk assessment tools.

For the purpose of modeling, it is important to know when overland flow will most likely become concentrated. As can be seen from the results of this study, the formation of concentrated flow increases the risk of erosion by increasing the total shear stress. In addition, formation of concentrated flow reduces the impact of cover for protecting the soil. Equation 14 can be used to predict the probability of concentrated flow formation using slope, bare soil fraction, and unit flow discharge. Slope and fraction of bare soil can be measured in the field, while flow discharge can be obtained from a hydrologic model of overland flow. Once a probability of concentrated flow formation is calculated, researchers can assume that the probability value is equal to the portion of overland flow that would be concentrated. After that, equation 18 can be applied to this portion of overland flow in order to estimate the effective shear stress fraction by concentrated flow. In the case that Darcy-Weisbach friction is needed for estimating flow discharge, researchers can use equation 23. The flow discharge resulting from equation 23 can be then used in equation 14 for distributing flow into concentrated flow or sheet flow. If differentiation between concentrated flow and sheet flow is not important, then equations 22 through 25 can be used as an approximation of the hydraulics and shear stress partitioning.

For the purpose of risk assessment modeling, researchers can use equation 14 for estimating the risk of concentrated flow formation in a specific scenario for a selected site. An assessment of how well that site is protected against such concentrated flow can be investigated using the shear stress partitioning equations in table 3. Figure 12 shows an example of risk index calculated from equations 14 and 18 for the scenario of q = 0.0009 m^2 s^{-1} (i.e., average value of q in this study). The risk index represents the possibility of flow to concentrate and how much the shear stress due to such concentrated flow would be effective for generating erosion. Picking an arbitrary threshold value for a site with a slope of 0.15 being at risk when the risk index is equal to 0.1, a rangeland site would be at risk if bare soil exceeded 60%. It is important to mention here that the risk index is for a specific scenario where q = 0.0009 m^2 s^{-1}. In order to have more realistic risk assessment, the risk of having high values of q must be established and then combined with the risk index shown in figure 12. Several factors control the value of q, including rainfall intensity and duration, slope, and vegetation cover. Since vegetation cover reduces q by adding more hydraulic friction to flow and increasing infiltration

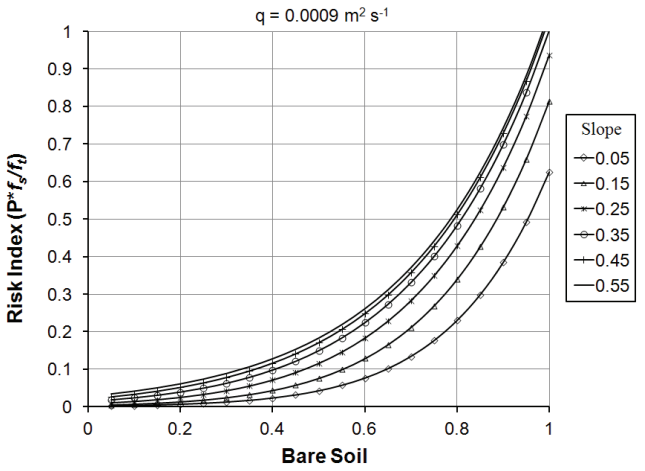

Figure 12. Risk index of possible higher erosion rate in the case of overland unit flow discharge of q = 0.0009 m^2 s^{-1} on rangeland as a function of bare soil and slope. The risk index is a result of the probability of flow to concentrate (P) times the shear stress fraction using equation 18 (f_f/f_t).

rate, the threshold value of bare soil at which the site would be at risk can be higher if the q value has less chance of being achieved at this bare soil value. For instance, if a site with slope of 0.15 has a high chance of producing a q value of 0.0009 m^2 s^{-1} only if bare soil exceeds 80%, then the threshold value of bare soil at which the site is at risk would be larger than 60%.

SUMMARY AND CONCLUSIONS

In this study, the effective shear stress component was estimated based on the assumption that the ratio of effective shear stress to total shear stress is equal to the ratio of hydraulic friction factor of the soil to the friction factor of the composite surface. The total hydraulic friction factor was obtained from empirical equations developed by regressing the measured total friction against measured vegetation and rock cover, slope, and flow rate. The hydraulic friction factor of each cover element was estimated based on its parameter in the respective equation. Empirical equations that predict the ratio of effective shear stress to total shear stress in terms of bare soil area were developed. The equations are applicable across a wide range of ecological sites, soils, slopes, and vegetation and ground cover conditions and can be used by physically based rangeland hydrology and erosion models. A logistic equation was developed to estimate the probability of overland flow to become concentrated. This study shows that shear stress exerted on soil grains estimated by the developed partitioning equations was relatively small in sheet flow. Shear stress exerted on soil grains, as estimated by the developed partitioning equations, is significantly lower when bare soil is less than 25% and significantly higher when bare soil exceeds 60% of the total surface area or when the plant basal cover is less than 20%. The logistic equation that estimates the chances of overland flow to become concentrated and the above-mentioned percentages could be used as relative measures of hydrologic recovery for disturbed rangelands or as triggers that indicate a site is crossing a threshold beyond which soil

erosion might accelerate due to the high effective shear stress.

ACKNOWLEDGEMENTS

This research was funded in part by the USDA-NRCS/ARS Conservation Effects Assessment Project (CEAP) and the U.S. Joint Fire Sciences program. This article is contribution No. 61 of the Sagebrush Steppe Treatment Evaluation Project (SageSTEP), funded by the U.S. Joint Fire Science Program. The USDA is an equal opportunity provider and employer.

REFERENCES

Abrahams, A. D., A. J. Parsons, and J. Wainwright. 1995. Effects of vegetation change on interrill runoff and erosion, Walnut Gulch, southern Arizona. *Geomorphology* 13(1-4): 37-48.

Al-Hamdan, O. Z., F. B. Pierson, M. A. Nearing, J. J. Stone, C. J. Williams, C. A. Moffet, P. R. Kormos, J. Boll, and M. A. Weltz. 2012. Characteristics of concentrated flow hydraulics for rangeland ecosystems: Implications for hydrologic modeling. *Earth Surf. Proc. Landforms* 37(2): 157-168.

Allison, P. D. 1999. *Multiple Regression: A Primer.* Thousand Oaks, Cal.: Pine Forge Press.

Blackburn, W. H. 1975. Factors influencing infiltration and sediment production of semiarid rangelands in Nevada. *Water Resour. Res.* 11(6): 929-937.

Einstein, H. A., and R. B. Banks. 1950. Fluid resistance of composite roughness. *Eos Trans. AGU* 31(4): 603-610.

Einstein, H. A., and N. L. Barbarossa. 1952. River channel roughness. *Trans. ASCE* 117: 1121-1132.

Flanagan, D. C., and M. A. Nearing, eds. 1995. *USDA Water Erosion Prediction Project: Hillslope Profile and Watershed Model Documentation*. NSERL Report No. 10. West Lafayette, Ind.: USDA-ARS National Soil Erosion Research Laboratory.

Foster, G. R. 1982. Modeling the erosion process. In *Hydrologic Modeling of Small Watersheds*, 295-382 C. T. Haan, H. P. Johnson., and D. L. Brakensiek, eds. ASAE Monograph No. 5: St. Joseph, Mich.: ASAE.

Foster, G. R., L. J. Lane, J. D. Nowlin, J. M. Laflen, and R. A. Young. 1980. A model to estimate sediment yield from field-sized areas: Development of model. In *CREAMS: A Field-Scale Model for Chemicals, Runoff, and Erosion from Agricultural Management Systems: Vol. 1. Model Documentation*, 36-64. Conservation Research Report No. 26. Washington, D.C.: USDA Science and Education Administration.

Foster, G. R., C. B. Johnson, and W. C. Mouldenhauer. 1982. Hydraulics of failure of unanchored cornstalk and wheat straw mulches for erosion control. *Trans. ASAE* 25(4): 940-947.

Gifford, C. F. 1985. Cover allocation in rangeland watershed management: A review. In *Proc. ASCE Symp.: Watershed Management in the Eighties*, 23-31. Reston, Va.: ASCE.

Gilley, J. E., and M. A. Weltz. 1995. Chapter 10: Hydraulics of overland flow. In *USDA Water Erosion Prediction Project: Hillslope Profile and Watershed Model Documentation*. D. C. Flanagan and M. A. Nearing, eds. NSERL Report No. 10. West Lafayette, Ind.: USDA-ARS National Soil Erosion Research Laboratory.

Giménez, R., and G. Govers. 2008. Effects of freshly incorporated straw residue on rill erosion and hydraulics. *Catena* 72(2): 214-223.

Hu, S. X., and A. D. Abrahams. 2006. Partitioning resistance to overland flow on rough mobile beds. *Earth Surf. Proc. Landforms* 31(10): 1280-1291.

Laursen, E. M. 1958. The total sediment load of streams. *J. Hydraulics Div. ASCE* 84(1): 1-36.

Li, G. 2009. Preliminary study of the interference of surface objects and rainfall in overland flow resistance. *Catena* 78(2): 154-158.

Ludwig, J. A., B. P. Wilcox, D. D. Breshears, D. J. Tongway, and A. C. Imeson. 2005. Vegetation patches and runoff-erosion as interacting ecohydrological processes in semiarid landscapes. *Ecology* 86(2): 288-297.

Moffet, C. A., F. B. Pierson, P. R. Robichaud, K. E. Spaeth, and S. P. Hardegree. 2007. Modeling soil erosion on steep sagebrush rangeland before and after prescribed fire. *Catena* 71(2): 218-228.

Nearing, M. A., G. R. Foster, L. J. Lane, and S. C. Finkner. 1989. A process-based soil erosion model for USDA Water Erosion Prediction Project technology. *Trans. ASAE* 32(5): 1587-1593.

Parsons, A. J., A. D., Abrahams, and J. Wainwright. 1996. Responses of interrill runoff and erosion rates to vegetation change in southern Arizona. *Geomorphology* 14(4): 311-317.

Pierson, F. B., J. D. Bates, and T. J. Svejcar, and S. P. Hardegree. 2007. Runoff and erosion after cutting western juniper. *Rangeland Ecology Mgmt.* 60(3): 285-292.

Pierson, F. B., W. H. Blackburn, S. S. Van Vactor, and J. C. Wood. 1994. Responses of interrill runoff and erosion rates to vegetation change in southern Arizona. *Water Res. Bull.* 30(6): 1081-1089.

Pierson, F. B., P. R. Robichaud, C. A. Moffet, K. E. Spaeth, S. P. Hardegree, P. E. Clark, and C. J. Williams. 2008a. Fire effects on rangeland hydrology and erosion in a steep sagebrush-dominated landscape. *Hydrol. Proc.* 22(16): 2916-2929.

Pierson, F. B., P. R. Robichaud, C. A. Moffet, K. E. Spaeth, C. J. Williams, S. P. Hardegree, and P. E. Clark. 2008b. Soil water repellency and infiltration in coarse-textured soils of burned and unburned sagebrush ecosystems. *Catena* 74(2): 98-108.

Pierson, F. B., C. A. Moffet, C. J. Williams, S. P. Hardegree, and P. E. Clark. 2009. Prescribed-fire effects on rill and interrill runoff and erosion in a mountainous sagebrush landscape. *Earth Surf. Proc. Landforms* 34(2): 193-203.

Pierson, F. B., C. J. Williams, P. R. Kormos, S. P. Hardegree, and P. E. Clark. 2010. Hydrologic vulnerability of sagebrush steppe following pinyon and juniper encroachment. *Rangeland Ecology Mgmt.* 63(6): 614-629.

Pierson, F. B., C. J. Williams, S. P. Hardegree, M. A. Weltz, J. J. Stone, and P. E. Clark. 2011. Fire, plant invasions, and erosion events on western rangelands. *Rangeland Ecology Mgmt.* 64(5): 439-449.

Raupach, M. R. 1992. Drag and drag partition on rough surfaces. *Boundary-Layer Meteorol.* 60(4): 375-395.

SAS. 2007. *SAS for Windows.* Cary, N.C.: SAS Institute, Inc.

Temple, D. M. 1980. Tractive force design of vegetated channels. *Trans. ASAE* 23(4): 884-890.

Temple, D. M. 1983. Design of grass-lined open channels. *Trans. ASAE* 26(4): 1064-1069.

Temple, D. M. 1985. Stability of grass-lined open channels following mowing. *Trans. ASAE* 28(3): 750-754.

Thompson, A. M., B. N. Wilson, and B. J. Hansen. 2004, Shear stress partitioning for idealized vegetated surfaces. *Trans. ASAE* 47 (3): 701-709.

Weltz, M. A., A. B. Awadis, and L. J. Lane. 1992. Hydraulic roughness coefficients for native rangelands. *J. Irrig. Draining Eng. ASCE* 118(5): 776-790.

Wilcox, A. C., J. M. Nelson, and E. E. Wohl. 2006. Flow resistance dynamics in step-pool channels: 2. Partitioning between grain, spill, and woody debris resistance. *Water Resour. Res.* 42(5): W05419, doi: 10.1029/2005WR004278.

Wilcox, B. P., M. K. Wood, and J. M. Tromble. 1988. Factors influencing infiltrability of semiarid mountain slopes. *J. Range Mgmt.* 41(3): 197-206.

Wilcox, B. P., B. D. Newman, D. Brandes, D. W. Davenport, and K. Reid. 1997. Runoff from a semiarid Ponderosa pine hillslope in New Mexico. *Water Resour. Res.* 33(10): 2301-2314.